GEOMETRY OPTIMIZATION OF DC/RF PHOTOELECTRON GUN*

P. Chen#, R. Yi, D. Yu
DULY Research Inc, Rancho Palos Verdes, CA 90275, USA

Abstract

High gradient pre-acceleration of photoelectron in a pulsed high voltage, dc gap and its subsequent injection into an rf gun is a promising method to improve electron beam emittance in rf accelerators. Simulation work has been performed in order to improve beam properties by optimizing the geometric shapes of a cylindrically symmetric dc/rf gun. Variations were made on cathode and anode shapes, dc gap distance and anode iris length. Significant improvement on the normalized transverse emittance Xn (<<1 mm·mrad), was obtained, as compared to an rf gun only or dc guns with flat cathode, after the gun geometry was optimized.

INTRODUCTION

Space charge induced emittance growth in conventional rf electron guns is one of the major barriers in the development of advance photoinjectors. Fast emittance growth is severe near the cathode, where electron energy is low. RF electron guns manage to overcome the problem by using higher peak rf field, but the field is limited by available rf power and by voltage breakdown. To minimize the emittance degradation induced by space charges, researchers in Brookhaven National Lab (BNL) and elsewhere [1-4] suggested a novel structure, a small-gap dc gun which uses a short-pulse dc field much higher than the typical rf peak field in a photoinjector . Studies of dc voltage breakdown conducted by Juttner *et. al.* [6] and Mesyats *et. al.* [7], and more recently of rf breakdown in high-gradient linear colliders worldwide, confirm that metal surfaces can withstand a higher voltage at a shorter pulse duration. The dc/rf gun [5,8] uses a pulsed dc electric field to accelerate electrons quickly across a small gap between a negatively biased photocathode and the grounded backplane of an rf cavity, and then eject the electrons into an rf cavity for further acceleration.

In this paper, we present simulation results using SUPERFISH and PARMELA codes on dc/rf guns designed by DULY Research Inc. For the dc gun design, in addition to a flat diode [5], a Pierce-like gun with a curved anode and cathode [3,9] was studied in order to improve field shape and minimize the transverse emittance Xn. Beams with small Xn at the anode exit and the rf cavity exit were obtained by optimizing geometry shapes of the dc gap and the drift length through the anode iris.

DESCRIPTION OF THE DC/RF GUN

The dc/rf system includes a pulser, a transmission line, a dc gun, and an rf cavity (Fig. 1).

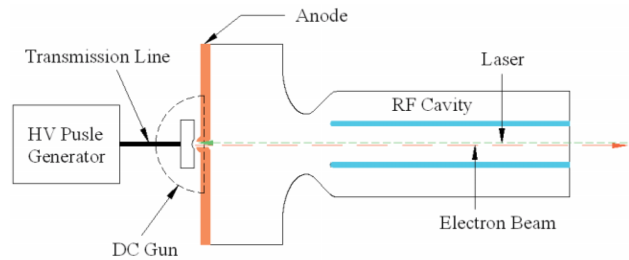

Fig. 1 Schematic diagram of an integrated dc/rf gun

Copper is chosen as the photocathode material because of its ease of preparation, relative insensitivity to contamination, long life, and fast response time. Another advantage is the reduction of work function in high field due to Schottky effect, which makes visible photon irradiation possible and may increase electron yield [3]. The cathode is biased at –500 KV with a 50 ps flat-top pulse. In principle this can be generated by a pulser producing a –250 KV, 100 ps flat-top pulse [5]. After dc acceleration, the electron beam is injected into an rf cavity. In collaboration with the Argonne National Laboratory (ANL), a test setup is under preparation using an existing 1-cell rf gun at the Injector Test Stand (ITS) [10]. The backplane of the coaxially coupled rf cavity can be retrofitted with an anode plate. The cavity has a built-in cathode canister which can mate to the DULY cathode and transmission assembly using a standard conflat flange. Photoelectrons are produced with an existing ANL laser. A photocathode radius of 0.5 mm is defined by the irradiating laser spot. Simulations assumed a bunch length of 5 ps and a bunch charge of 200 pC.

SIMULATIONS OF DC/RF GUN

RF Gun only

Simulations were first performed on an rf gun without a dc gap using SUPERFISH and PARMELA codes. The gun consists of only one cell (right side in Figure 1) operated at 2856 MHz. Calculations were made for different injection angles without solenoid focusing. Results are plotted in Fig. 2. At injection angle=7.4º, the smallest Xn achieved for this gun was 1.1 mm·mrad at 15 cm from the exit of the cavity (including the coax waveguide/drift tube), a point where measurement can be taken in actual tests (Point A). Although Xn value was small at this location, it rapidly increased as the distance increased (See Fig. 5). The root-mean-square (rms) transverse beam size (Xrms) was also as high as 4.1 mm.

*Work supported by U.S. Department of Energy SBIR grant no. DE-FG03-02ER83402
#pchen1@sbcglobal.net

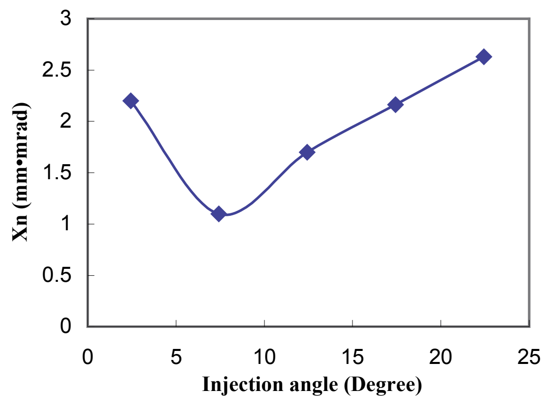

Fig. 2 Xn vs injection angle for a 1-cell rf gun.

DC/RF Guns

To improve electron beam properties further, a dc injection gun is planned to be installed before the rf cavity so that the initial injection energy of the electron beam can be much higher. Three different dc gun geometries were used in the studies. In order to describe the guns clearly, we give names to the guns as Type A, Type B, and Type C. Schematics of the guns are shown in Fig. 3.

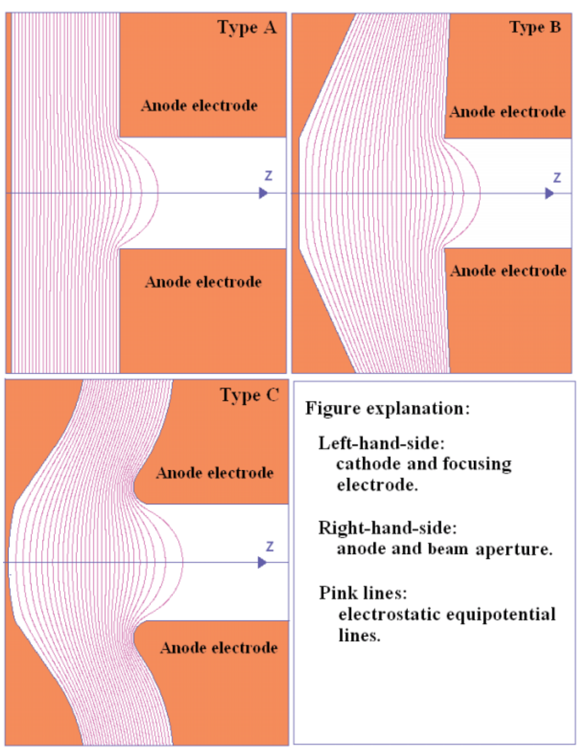

Fig. 3 Geometry shapes and equipotential lines of three dc guns.

Beam simulations started from the cathode at the dc gap, across the anode drift tube, and through the rf cavity. The challenging problem was to design a dc gun that would deliver an electron beam with a small Xn and a laminar beam envelope.

A simple dc flat diode (Type A) was simulated first as its geometry limitation was the easiest to understand. For an ideal, space-charge-limited, flat diode gun with a continuous beam, the perveance is 0.113 μPerv at 40 A (=200pC/5ps) and 500 KV, according to Child's law. In this case, the field on the cathode surface is 124 MV/m if the radius of circular photocathode emission area is 0.5 mm, assuming a uniform emitting current density. This implies that Zgap, the gap distance, can't be too large. We used the field value to size roughly the largest Zgap at the beginning of each simulation.

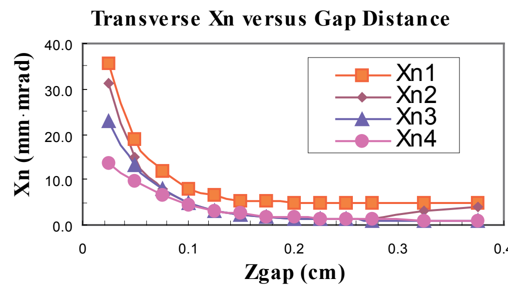

Fig. 4 Xn trends at the end of drift tube of Type A guns

Results of Xn as a function of Zgap at the end of drift tube of Type A gun are shown in Fig. 4, with an anode electrode thickness of 5 mm, and anode aperture radius of ra=0.5, 0.55, 0.75, 1mm (corresponding to Xn1 through Xn4, respectively). Apparently contrary to the common view that a high field gradient should induce a low Xn, it was found that Xn would decrease when field gradient became lower for the Type A gun. Detailed investigations showed that the emittance dilution consisted of two parts: the first part was induced by space charge effect and the second part by electric field distortion. When ra was comparable to Zgap, large E-field distortion, mainly caused by the anode aperture, would blow up the beam transverse emittance when the beam entered the aperture. We could raise the axial field gradient to suppress the space charge effects, but the distorted field would increase the transverse emittance. Thus, for the Type A dc gun, two geometry changes could benefit the control of Xn growth: large Zgap or large ra. These two parameters were varied in the simulations of the Type A gun. But the maximum changes of Zgap and ra were limited by cathode surface E-fields, i.e. the larger Zgap or ra, the weaker the field. We found that the smallest Xn was around 1 mm·mrad at the exit of a Type A gun. However, a beam obtained from such gun diverged very fast as it was injected into an rf cavity for further acceleration. Table 1 lists the beam properties at Point A beyond the Type A gun and the rf cell. Because of the beam divergence in the dc gun, a portion of the beam hit the wall of the anode drift tube, which would heat the anode and reduce beam current in actual operations. Though cutting iris length was helpful to avoid more particles hitting the wall, the length could not be shorter than 3 mm. Otherwise, rf power would leak out seriously from the cavity to the dc gun gap through the aperture. Results here revealed that Type A gun was not ideal to get high quality beam.

To improve Xn and Xrms, flat guns using focusing electrode (Type B) were simulated. Three sensitive geometry parameters were chosen as variables because they affected Xn and Xrms most. They were (1) Zgap, (2) focusing angle (α), an angle that the focusing electrode makes with the normal cathode surface, and (3) anode angle, an angle between the anode electrode and beam axis. The beam with the smallest Xn from dc guns was then injected into the rf cavity. Beam properties at Point A were obtained and illustrated in Table 1. Though great improvement was made compared to the beam properties from the Type A dc/rf gun, Type B seemed still not quite good enough because the beam from it spread too fast in the simulations. Considering the high current density (~5100A/cm^2) on the photocathode in our guns, we realized that an initial converging angle would be necessary for electrons when they formed a beam. The angle might help the beam to counteract the strong defocusing force in the accelerating gap. In addition, a curved anode would be good to modify the field near the anode.

Table 1. Comparison for different guns

Gun Type	Xn (mm·mrad)	Xrms (mm)	Zn (mm·mrad)	Zrms (mm)	E* (MeV)
RF gun	1.10	4.2	4.87	0.56	2.89
Type A+ rf cell	1.02	4.4	4.75	0.5	3.40
Type B+ rf cell	0.82	2.11	7.51	0.49	3.47
Type C+ rf cell	0.27	1.72	10.63	0.48	3.46

E*: Final beam energy

Among guns with curved cathode and curved anode (Type C), we found that the Pierce gun was one of the best choices because there were design formulas [11] to calculate the important geometry parameters such as cathode curvature radius (Rc), anode curvature radius (Ra), and etc. We guessed that the optimized parameters of Type C might be around the values given by the Pierce formulas for a given beam perveance. The simulations following confirmed our thoughts. Results in Table 1 indicate that Xn from an optimized Type C + rf cell gun was only 0.27 mm·mrad, while its Xrms was 1.72 mm at Point A. Fig. 5 plots the Xn variations of all guns described above. The curve for Type C gun (Fig. 5) shows that the beam quality has improved remarkably compared to the results of the other two types of guns. The optimized geometry parameters for Type C+rf cell gun are listed in Table 2.

Table 2. Parameters for an optimized Type C gun

Parameter	Zgap (mm)	Rc (mm)	α (degree)	Ra (mm)	Anode iris length (mm)	β** (degree)
Values	1.91	4.46	67.50	2.34	4.09	20.35

** Injection phase

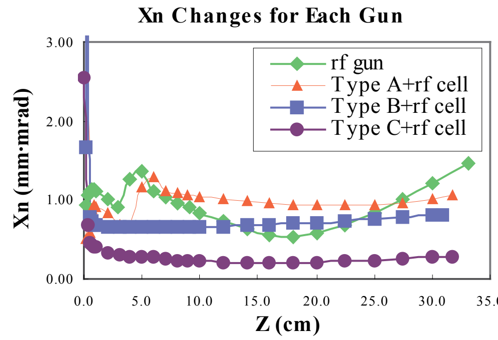

Fig. 5 Xn variations for each type of the guns

Dependency and sensitivity of beam quality with respect to geometry changes were also investigated for Type C. Results of the simulations are shown in Table 3.

Table 3. Sensitivity for the optimized gun

Parameter changed	Value changed	Xn (mm·mrad)	Xrms (mm)	Zn (mm·mrad)	Zrms (mm)	E (MeV)
Zgap (mm)	-0.1	0.01	0.03	-0.47	-0.02	-0.04
	0.1	0.13	-0.11	0.81	0.00	-0.04
Rc (mm)	-0.2	0.10	-0.10	0.72	-0.01	-0.04
	0.2	0.03	0.01	-0.23	-0.01	-0.04
α (degree)	-2.5	0.08	-0.09	0.62	-0.01	-0.04
	2.5	0.03	0.00	-0.19	-0.01	-0.04
Ra (mm)	-0.1	0.18	-0.15	1.30	0.00	-0.03
	0.1	0.03	0.16	-1.46	-0.02	-0.04
Iris length (mm)	-0.5	0.05	-0.04	0.12	-0.01	-0.04
	0.5	0.03	0.03	-0.29	-0.01	-0.04
β (degree)	-5	0.04	-0.01	-0.09	-0.01	-0.04
	5	-0.01	0.02	0.04	0.01	0.01

REFERENCES

[1] T. Srinivasant-Rao, et al., AAC workshop, AIP Conference Proceedings 398, NY 1997, P. 7307.

[2] T. Srinivasan-Rao, et al., J.Opt. Soc. Am.B8, p294, 1991; F. Villa, AAC96, Lake Tahoe, AIP398, pp.739-746, 1997.

[3] K. Batchelor, et al., 6th EPAC, June 22-26, 1998, Stockholm, Sweden. P. 791.

[4] F. Zhou, et al., PAC 2001, Chicago, P. 2266-2268.

[5] D. Yu, et al., PAC 2003, Portland, P. 2132-2134, May 12-16, 2003.

[6] B. Juttner, et al., Proc. iii Int'l Symp. on Discharge and Electrical Insulation in Vacuum, Paris, France, 1968, p. 209.

[7] G. A. Mesyats, et al., Pulsed Electrical Discharge in Vacuum, (Springer-Verlag, 1989), Chap 1-5.

[8] M. J. van der Wiel, Proc. 2nd ICFA Adv. Acc. Workshop, UCLA, Nov. 1999; S.B. van der Geer, et al., Phys. Rev. E, Vol 65, 046501 (2002).

[9] T. Srinivasan-Rao, et al., BNL 65748 ; pres. 8th Workshop on AAC, Baltimore, MD, 6-11 July (1998); AIP Conf. Proc. 472 (1999), Wes Lawson, ed.

[10] J. Lewellen, private communication.

[11] J. R. M. Vaughan, IEEE Trans. Electron Devices, vol. ED-28, no 1, Jan. 1981.